Journal of the Indian Chemical Society 103 (2026) 102847

Contents lists available at ScienceDirect

Journal of the Indian Chemical Society

journal homepage: www.journals.elsevier.com/journal-of-the-indian-chemical-society

Influence of tungsten content on the electrochemical performance of $CuWO_4$ nanoparticles for supercapacitor applications

S. Umera Sulthana [a], D. Sridevi [b], V. Balasubramanian [c], B. Shunmugapriya [d], A. Alfind Paul Frit [e], V. Gowthami [a,*]

[a] Department of Physics, School of Basic Sciences, Vels Institute of Science, Technology and Advanced Studies, Chennai, Tamil Nadu, 600117, India
[b] Department of Physics, Prathyusha Engineering College (Autonomous), Tiruvallur, Tamil Nadu, 602025, India
[c] Department of Physics, SRM Institute of Science and Technology, Ramapuram, Chennai, Tamil Nadu, 600089, India
[d] Department of Physics, S. A. Engineering College (Autonomous), Chennai, Tamil Nadu, 600077, India
[e] Department of Physics, Vel Tech High Tech Dr.Rangarajan Dr.Sakunthala Engineering College (Autonomous), Chennai, Tamil Nadu, 600062, India

ARTICLE INFO

Keywords:
$CuWO_4$
Sol-gel
Pseudocapacitor
Raman spectra
Charge transfer

ABSTRACT

The influence of composition on the physicochemical properties and electrochemical performance of $CuWO_4$ nanoparticles with various tungsten contents synthesized by a sol-gel method was investigated for supercapacitor applications. X-ray diffraction confirmed the formation of crystalline CuWO4 while the characteristic Cu–O and W–O vibrations were observed by Raman spectroscopy. SEM-EDX analysis showed uniform morphology and suitable elemental composition. The electrochemical studies using cyclic voltammetry and galvanostatic charge discharge techniques revealed pseudocapacitive behavior due to reversible Cu^{2+}/Cu^{+} and W^{6+}/W^{5+} redox reactions. The $CuWO_4$ (1:1) sample showed the highest specific capacitance of 204.5 F g^{-1} at 0.25 A g^{-1} due to its optimized Cu–O–W framework, higher electroactive surface area, and improved charge transport. These results highlight the critical role of tungsten content in tuning structure-property relationships and demonstrate the potential of $CuWO_4$ nanoparticles as efficient electrode materials for supercapacitor applications.

1. Introduction

The need for effective and sustainable energy storage systems has increased because of the quick development of portable devices, electric cars, and renewable energy technologies. When compared to traditional batteries, supercapacitors exhibit superior cycling stability, high power density, and quick charge-discharge performance [1,2]. The development of electrodes with high specific capacitance, excellent electrical conductivity, and long-term chemical stability is necessary because of their relatively low energy density, which is still a major problem and is mostly caused by the inherent characteristics of electrode materials [3]. Electrostatic charge accumulation at the electrode–electrolyte interface or quick, reversible faradaic redox reactions are the two methods for charge storage in supercapacitors. Although the rate capability and cycling stability of carbon-based electric double-layer capacitor materials are higher, the energy storage capacity is limited in nature. In contrast, pseudocapacitive materials can increase the energy density by using surface or near-surface redox reactions that involve several oxidation states. Pseudocapacitive electrode materials based on transition metal oxides have attracted much interest due to their rich redox chemistry and structural flexibility. [4,5]. Other transition metal oxides have attracted much attention as supercapacitor materials such as transition metal tungstates MWX_4 (M = transition metal; X = W or Mo). Compared with the single metal oxides, these materials show enhanced charge storage ability due to the synergistic electrochemical activity of the two different metal cations. Copper tungstate ($CuWO_4$) has received much attention because of its high theoretical capacitance, structural stability, cheap and eco-friendly nature [6,7]. $CuWO_4$ is a good electrode material for cutting-edge energy storage devices because of its bimetallic character, which allows for the effective use of redox-active sites. The monoclinic wolframite-type crystal structure of $CuWO_4$ is composed by CuO_4 and WO_4 octahedra that share edges [8]. During charge-discharge cycles, this networked structure offers a large number of electrochemically active sites and promotes effective ion diffusion [9]. While W^{+} ions improve structural stability and can take part in further redox processes under appropriate electrochemical conditions, Cu^{2+} ions with a d^1 electronic configuration experience reversible Cu^{2+}/Cu^{3+} redox transitions that greatly contribute to

* Corresponding author.
E-mail address: gowthamivijayakumar@gmail.com (V. Gowthami).

https://doi.org/10.1016/j.jics.2026.102847
Received 3 April 2026; Received in revised form 17 June 2026; Accepted 27 June 2026
Available online 27 June 2026
0019-4522/© 2026 Published by Elsevier B.V. on behalf of Indian Chemical Society.

pseudocapacitive behavior [10]. Consequently, $CuWO_4$-based electrodes have demonstrated excellent cycling stability with retention rates over 85% for prolonged charge-discharge cycles, as well as high specific capacitance values, reaching over 600 F g^{-1} in nanostructured forms [11]. $CuWO_4$ morphology, crystallinity, and particle size all of which are primarily determined by the production process have a significant impact on its electrochemical performance. High surface area, shorter ion diffusion paths, and enhanced electrolyte accessibility are all provided by nanostructured $CuWO_4$ structures, which improve electrochemical kinetics [12,13]. The sol-gel process has several advantages over other synthesis process, such as reduced processing temperature, better compositional consistency, and control of particle size and microstructure. Additionally, very uniform and phase-pure $CuWO_4$ nanoparticles may be formed using the sol-gel approach, which is advantageous for obtaining repeatable and improved electrochemical performance [14,15]. Recent studies have demonstrated that the electrochemical performance of transition metal oxide-based electrode materials is strongly governed by their composition and physicochemical characteristics. For instance, previous reports have highlighted that variations in composition and nanostructure significantly influence charge storage mechanisms and ion transport behavior in energy storage systems [16,17]. Furthermore, the stoichiometric balance and reactant molar ratios play a crucial role in determining crystallinity, morphology, and charge-transfer kinetics, thereby directly affecting the overall electrochemical performance of these materials [18].

Despite these benefits, $CuWO_4$ relatively poor intrinsic electrical conductivity ($\sim 10^{-1}$ S cm^{-1}), which negatively impacts charge transfer kinetics and rate capabilities, nevertheless limits its practical deployment [19]. Techniques like surface modification, heteroatom doping, and compositing with conductive carbon materials have been extensively studied to get around this restriction [20]. $CuWO_4$ based composites containing graphene or carbon nanotubes, in particular, show synergistic effects that improve specific capacitance, electrical conductivity, and cycling stability [21–23]. These advancements demonstrate the ongoing potential for high-performance supercapacitor applications of $CuWO_4$-based materials produced using regulated processes like the sol–gel technique.

2. Materials and methods

Copper(II) nitrate trihydrate [$Cu(NO_3)_2{\cdot}3H_2O$] and sodium tungstate dihydrate [$Na_2WO_4{\cdot}2H_2O$] of analytical grade were used as copper and tungsten precursors without further purification, while polyvinylpyrrolidone (PVP) served as a growth-controlling agent. Deionized water was used as the solvent throughout the synthesis. Copper tungstate ($CuWO_4$) nanoparticles with Cu:W molar ratios of 1:1, 1:2, and 1:3 were synthesized via a sol–gel method. In a typical procedure, the required amount of copper(II) nitrate trihydrate was dissolved in deionized water under continuous magnetic stirring, and sodium tungstate dihydrate was dissolved separately with the addition of PVP. The tungstate solution was added dropwise to the copper precursor under constant stirring, followed by adjustment of the solution pH to approximately 7–9 using dilute ammonia to promote controlled nucleation and gel formation. The reaction mixture was further stirred and mildly heated to improve compositional homogeneity. The resulting product was collected by centrifugation, thoroughly washed with deionized water and ethanol to remove residual ions and organic species, and dried at 70 °C. Finally, the dried powder was calcined at 500 °C in air to obtain phase-pure and crystalline $CuWO_4$ nanoparticles suitable for structural, morphological, and electrochemical energy storage applications.

3. Preparation of electrode

The working electrode was prepared by mixing the as-synthesized $CuWO_4$ active material, conductive carbon black, and polyvinylidene fluoride (PVDF) binder in a weight ratio of 80:10:10 using N-methyl-2-pyrrolidone (NMP) as solvent to form a homogeneous slurry. The slurry was uniformly coated onto a cleaned nickel foam current collector (1×1 cm^2), followed by drying at 80 °C for 12 h in a hot air oven. The average mass loading of the active material was 2, 3 and 4 mg cm^{-2} for 1:1, 1:2, and 1:3 ratios respectively. Electrochemical measurements were carried out in a standard three-electrode configuration using 1 M KOH aqueous solution as the electrolyte. The prepared $CuWO_4$ electrode served as the working electrode, while a platinum wire and Ag/AgCl electrode were used as the counter and reference electrodes, respectively. Cyclic voltammetry (CV), galvanostatic charge–discharge (GCD), and electrochemical impedance spectroscopy (EIS) measurements were performed using an electrochemical workstation at room temperature.

4. Results and discussion

The formation of monoclinic $CuWO_4$ with distinctive diffraction peaks like (010), (100), (011), (110), (−111), (111), (021), and (002) is confirmed by the XRD patterns of $CuWO_4$ nanoparticles (Fig. 1) produced by the sol–gel method at various Cu:W ratios (1:1, 1:2, and 1:3). However, the crystallinity is highly dependent on stoichiometry. Due to balanced Cu^{2+} and WO_4^{2-} interaction, the 1:1 sample shows sharp, intense peaks that indicate well-developed crystallinity and proper phase formation, whereas the 1:2 sample shows moderately broadened and less intense peaks that suggest reduced crystallinity and potential lattice distortion from excess tungsten. Poor crystallinity, reduced crystallite size, and partial amorphous character are indicated by the 1:3 sample's peaks being noticeably broader with lower intensity and more background noise, most likely as a result of excess W inhibiting crystal growth. Overall, increasing tungsten content leads to decreased crystallinity, increased structural disorder, and reduced particle size, making the 1:1 ratio the most favorable for forming well-crystallized $CuWO_4$ nanoparticles.

The Raman spectra of $CuWO_4$ nanoparticles prepared by varying the tungsten ratios as shown in Fig. 2. The low-frequency modes below 300 cm^{-1} are attributed to lattice vibrations involving Cu–O–W linkages, the intermediate bands in the 300–700 cm^{-1} region originate from O–W–O bending modes, and the prominent high-frequency band observed around 900 cm^{-1} corresponds to the symmetric stretching vibrations of W–O bonds within WO_3 octahedra [24,25]. The stoichiometric $CuWO_4$ (1:1) sample displays sharper and more intense Raman peaks, reflecting superior crystallinity and a well-ordered Cu–O–W framework. Samples with excess tungsten (1:2 and 1:3) show

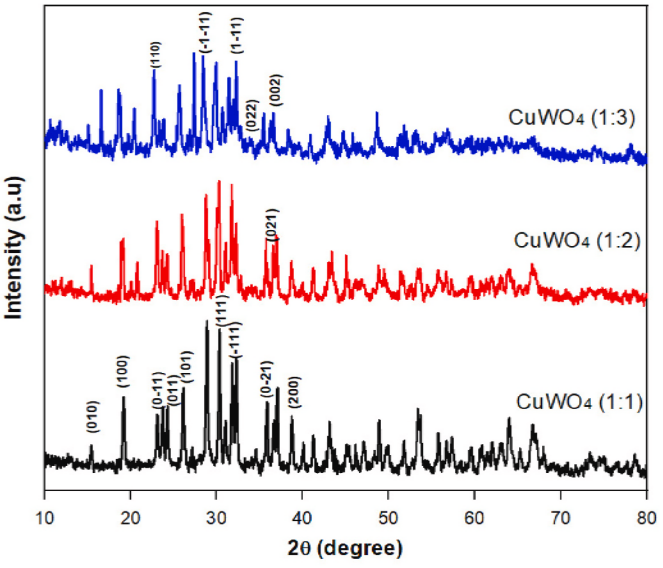


Fig. 1. XRD pattern of $CuWO_4$ nanoparticles.

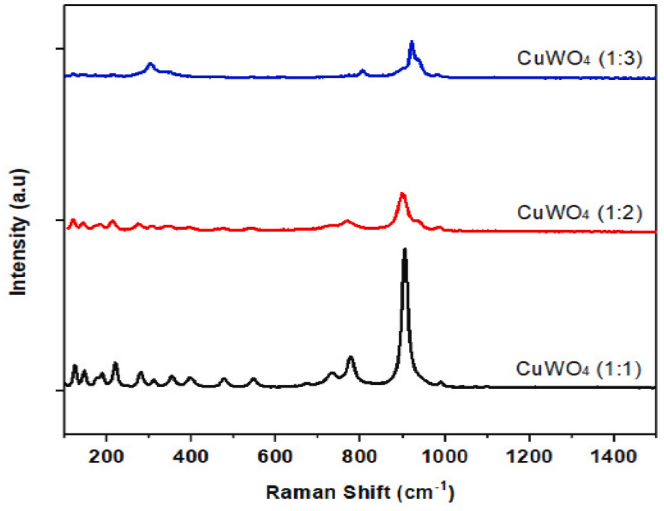


Fig. 2. Raman Spectra of $CuWO_4$ nanoparticles.

progressively broadened peaks, decreased intensity, and small shifts in the W–O stretching mode, which suggest increased lattice distortion, a higher density of defects, and phonon confinement effects caused by the extra tungsten. These findings are consistent with previous Raman studies on monoclinic $CuWO_4$ and related tungstate systems [26], suggesting that deviations from stoichiometric composition can distort the local WO_6 octahedral environment and reduce long-range structural order.

The SEM micrographs of $CuWO_4$ nanoparticles made with various tungsten ratios are displayed in Fig. 3. Agglomerated but comparatively uniform nanoparticles with a rough surface roughness are seen in the $CuWO_4$ (1:1) sample (Fig. 3a and b), suggesting homogeneous nucleation and good crystallinity. The particles become more densely packed with irregular morphologies and greater agglomeration when the tungsten content is increased to a Cu:W ratio of 1:2 (Fig. 3c and d). This suggests enhanced growth of grains and local structural distortion caused by excess W species. Larger, plate-like, highly aggregated structures with decreased porosity are formed when tungsten concentration is further increased to a Cu:W ratio of 1:3 (Fig. 3e and f). This can be explained by uncontrolled particle development and coalescence caused by tungsten-rich circumstances. The observed morphological evolution with increasing W ratio suggests that tungsten content is a key factor in controlling $CuWO_4$ nanoparticle aggregation behavior, surface roughness, and particle size. According to previous works on tungstate-based nanomaterials [27,28], such alterations in surface morphology and microstructure are anticipated to have a substantial impact on charge transport and electrochemical performance (see Fig. 4).

The elemental composition of the sample is confirmed by the Energy Dispersive X-ray Spectroscopy (EDAX) examination as shown in Fig. 4, which displays significant peaks corresponding to copper (Cu), tungsten (W), and oxygen (O). High purity is confirmed by the quantitative elemental analysis, which shows a near-stoichiometric ratio of Cu to W that is compatible with the chemical formula $CuWO_4$. No notable impurity peaks are seen. Additionally, the intensity of the corresponding signals in the spectra indicates that $CuWO_4$ is W rich. A thorough grasp of the surface morphology and elemental purity is provided by the combination of SEM and EDAX data, which is essential for assessing the material's applicability in uses like supercapacitors.

The XPS analysis of $CuWO_4$ confirms the successful formation of the material and provides insight into its oxidation states as shown in Fig. 5. The survey spectrum reveals the presence of Cu, W, and O elements without detectable impurities. The high-resolution Cu 2p spectrum shows characteristic peaks at 931.37 eV (Cu $2p_3/_2$) and 952.86 eV (Cu $2p_1/_2$), along with pronounced shake-up satellite peaks in the 940–945 eV and 961.22 eV regions, confirming the dominant presence of Cu^{2+} with a possible minor Cu^{+} contribution due to slight peak asymmetry, consistent with reported literature [29]. The W 4f spectrum exhibits two distinct peaks at 34.45 eV and 36.57 eV, corresponding to W $4f_7/_2$ and W $4f_5/_2$, respectively, with a typical spin–orbit splitting of 2.1 eV, indicating the presence of W^{6+} in $CuWO_4$ [30]. Further, the O 1s peak generally consists of lattice oxygen at 529.60 eV and higher binding energy components at 531.20 eV associated with surface hydroxyl groups or oxygen vacancies, which are known to enhance electrochemical activity [31]. The coexistence of Cu^{2+}/Cu^{+} redox couples and the stable W^{6+} framework promotes efficient Faradaic reactions and electron transport, while oxygen vacancies provide additional active sites and facilitate ion diffusion, thereby improving the overall electrochemical performance, including specific capacitance and rate capability.

The cyclic voltammetry (CV) curves of $CuWO_4$ nanoparticles produced with various Cu:W molar ratios of 1:1, 1:2, and 1:3 are displayed in Fig. 6(a–c), acquired at scan rates ranging from 10 to 100 mVs^{-1} within a potential window of −0.6 to +0.6 V. Instead of ideal rectangular electric double-layer behavior, the CV profiles for all compositions show quasi-rectangular forms with discernible redox humps, suggesting that the charge storage mechanism is mostly pseudocapacitive in nature. Reversible faradaic processes associated primarily with the Cu^{2+}/Cu^{+} redox couple are responsible for the observed pseudocapacitive behavior of the $CuWO_4$ electrode. In addition, tungsten may contribute through surface or near-surface redox transitions involving W^{6+}/W^{5+}, as commonly reported for transition-metal tungstate systems [32]. With increasing scan rate, the enclosed area of the CV curves and the corresponding current response increase proportionally, indicating good rate capability and efficient ion/electron transport within the electrode material [33].

The CV study clearly shows that the electrochemical behavior is strongly dependent on the tungsten content. The $CuWO_4$ electrode with a 1:2 and 1:3 M ratio (Fig. 6b & c) shows a smaller enclosed CV area and a relatively lower current response, suggesting fewer electrochemically active sites and less effective charge-transfer kinetics. The 1:1 (Fig. 6a) sample, on the other hand, exhibits more anodic and cathodic currents with noticeably larger CV regions, indicating enhanced charge-storage capacity.

Increased redox activity, higher structural integrity, and superior electronic conductivity from an optimized Cu–O–W framework, which encourages quick faradaic reactions and effective electrolyte ion transport, are responsible for the 1:1 $CuWO_4$ improved electrochemical performance. These findings are consistent with previous research by Wang et al. and Liu et al., which showed that strong metal–oxygen interactions and several accessible oxidation states enhance tungsten-rich metal tungstates, resulting in superior pseudocapacitive behavior [34,35]. Additionally, it is clear that even at greater scan rates, CV curves show similar or higher current densities and well-retained morphologies, indicating strong structural integrity and good electrochemical reversibility. The nanoparticle-based $CuWO_4$ in this study maintains symmetric and stable CV loops, demonstrating the advantageous effect of nanoscale morphology and optimized composition [36]. In contrast, Zhang et al. reported distorted CV profiles with pronounced polarization at high scan rates for bulk $CuWO_4$. Overall, the CV analysis shows that adjusting the Cu:W ratio has a major impact on the pseudocapacitive performance of $CuWO_4$ nanoparticles, with the 1:1 composition showing the most promising electrochemical properties for supercapacitor applications.

The GCD curves of $CuWO_4$ nanoparticles with Cu:W ratios of 1:1, 1:2, and 1:3 recorded at various current densities are shown in Fig. 7(a–c). A pseudocapacitive charge-storage mechanism is confirmed by the non-linear charge-discharge profiles and small voltage plateaus seen in all electrodes. Good rate capability and electrochemical reversibility are indicated by the discharge time decreasing with increasing current density. The 1:1 composition has longer discharge times, indicating a

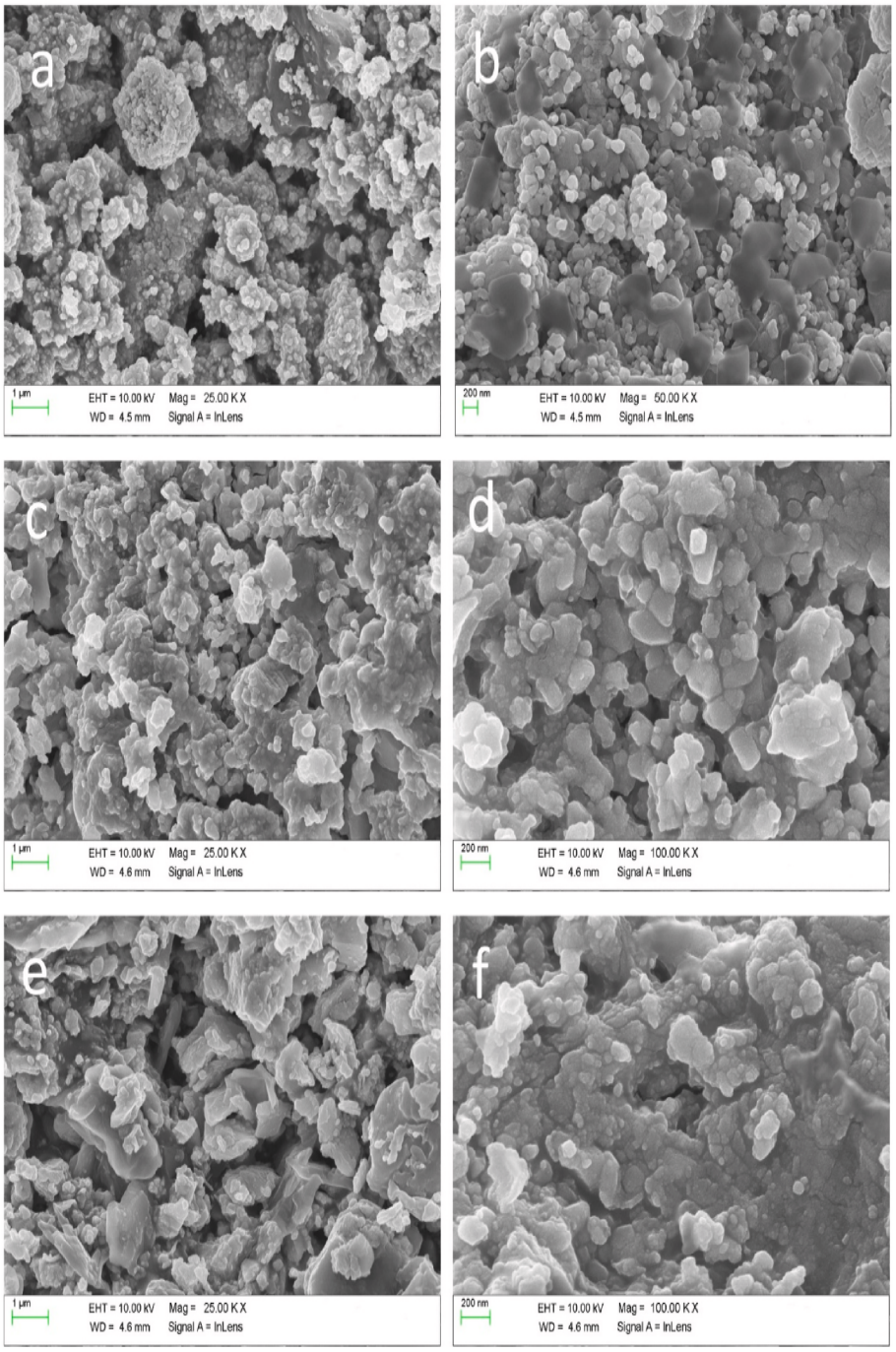


Fig. 3. SEM images of $CuWO_4$ nanoparticles (a,b) 1:1 (c,d) 1:2 (e,f) 1:3.

larger specific capacitance, whereas the 1:2 and 1:3 $CuWO_4$ samples show lower discharge durations. Increased redox-active sites and better ion/electron transport resulting from an optimized Cu–O–W framework are responsible for the 1:1 $CuWO_4$ improved performance. At all current densities, the $CuWO_4$ (1:1) sample (a) has the largest specific capacitance, delivering 204.5 F g^{-1} at 0.25 A g^{-1}, which progressively drops to 54.5 F g^{-1} at 5 A g^{-1} (Table 1). This sharp decline shows that ion diffusion constraints at higher current densities impact the material's performance even though it has a high density of electroactive sites and excellent charge storage capacity. The enhanced electrochemical performance of the $CuWO_4$ (1:1) sample can be attributed to its improved surface morphology, which provides a higher density of electroactive sites and facilitates efficient electrolyte ion diffusion. A similar correlation between morphological features and charge storage behavior has been reported in recent studies, where optimized nanostructures significantly improved pseudocapacitive performance [37]. The $CuWO_4$ (1:2) sample (b), on the other hand, has much reduced capacitance, stabilizing around 27–34 F g^{-1} at higher current densities and beginning at 47.7 F g^{-1} at 0.25 A g^{-1}. This comparatively flat trend indicates decreased conductivity and restricted ion accessibility, as well as limited faradaic activity but improved rate stability. Comparable starting capacitance of 45.5 F g^{-1} at 0.25 A g^{-1} is also shown by the $CuWO_4$ (1:3) sample (c), with values staying in the range of 25–36 F g^{-1} as current density increases. In comparison to the 1:2 composition, a notable improvement at greater current density (36.4 F g^{-1} at 5 A g^{-1}) indicates a more prevalent surface-controlled (pseudocapacitive) charge

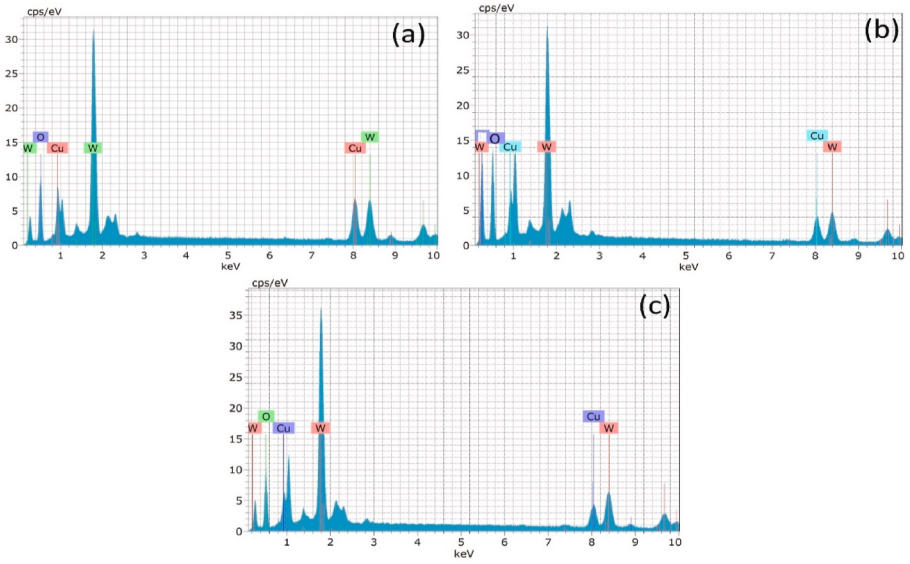


Fig. 4. EDAX spectra of $CuWO_4$ nanoparticles (a) 1:1 (b) 1:2 (c) 1:3.

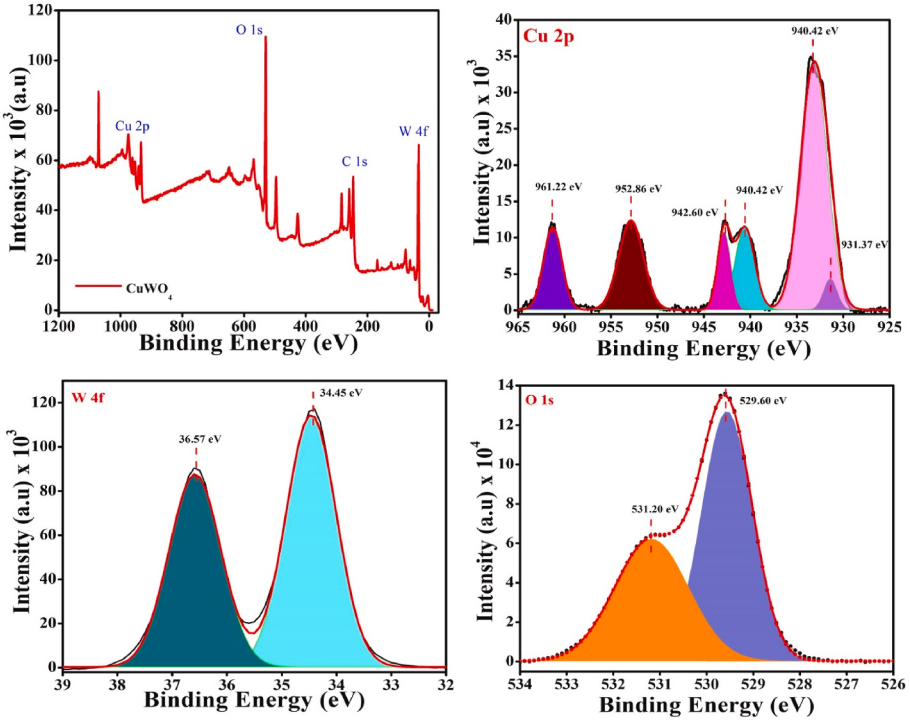


Fig. 5. XPS spectra of $CuWO_4$ nanoparticles.

storage mechanism and better rate capability. Herein, the observed decrease in capacitance for tungsten-rich compositions can be associated with reduced electrical conductivity and slower charge-transfer kinetics. This trend is consistent with recent reports highlighting that compositional imbalance can adversely affect electron transport and redox activity in transition metal oxides [38].

The superior performance of the 1:1 ratio (Fig. 8) can be initially attributed to an ideal balance between copper and tungsten species, resulting in enhanced electrical conductivity, more accessible active sites, and improved redox activity. In contrast, higher tungsten content in 1:2 and 1:3 ratios likely reduces conductivity and restricts effective charge storage.

The cycling stability of the $CuWO_4$ (1:1) electrode over 2000 charge–discharge cycles seen in Fig. 9 reveal an initial decrease in capacitance retention from 100% to 86% during the early cycles, which can be attributed to electrode activation, electrolyte penetration, and stabilization of the electrode/electrolyte interface. Following this initial drop, the capacitance gradually recovers and stabilizes, maintaining 92% retention up to 2000 cycles, indicating excellent electrochemical durability and structural integrity of the electrode material. Furthermore, the consistent and symmetric charge-discharge profiles shown in the inset demonstrating that the $CuWO_4$ (1:1) electrode is a promising candidate for long-term supercapacitor applications.

The electrochemical impedance spectroscopy (EIS) analysis of $CuWO_4$ (1:1) was performed to evaluate the charge transport and interfacial properties of the electrode, as shown in Fig. 10. The Nyquist

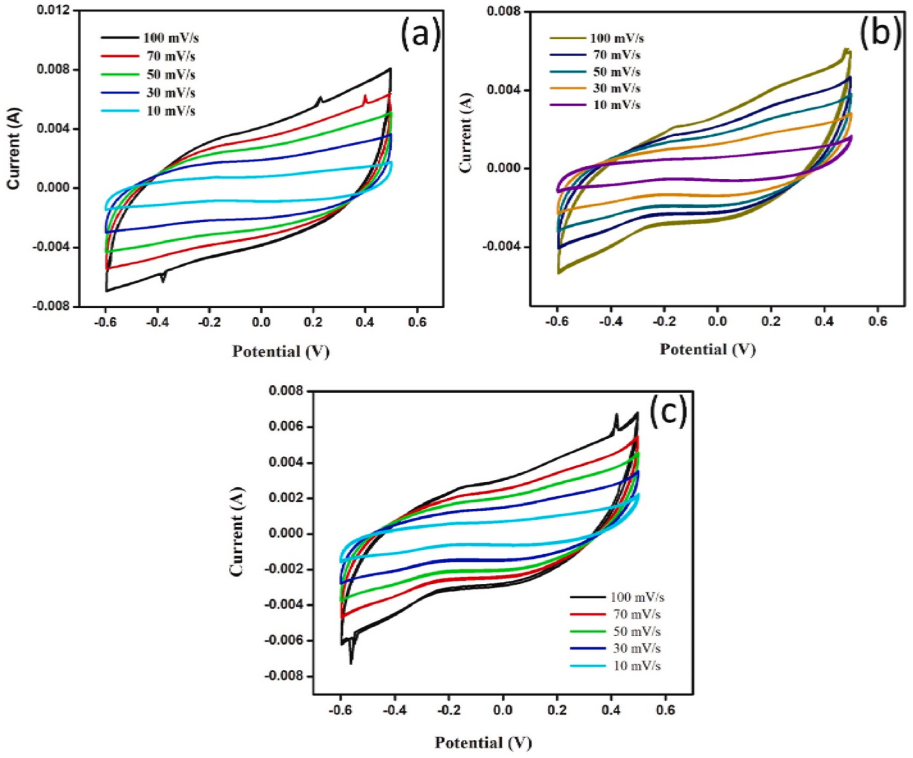


Fig. 6. CV curve of $CuWO_4$ nanoparticles (a) 1:1 (b) 1:2 (c) 1:3.

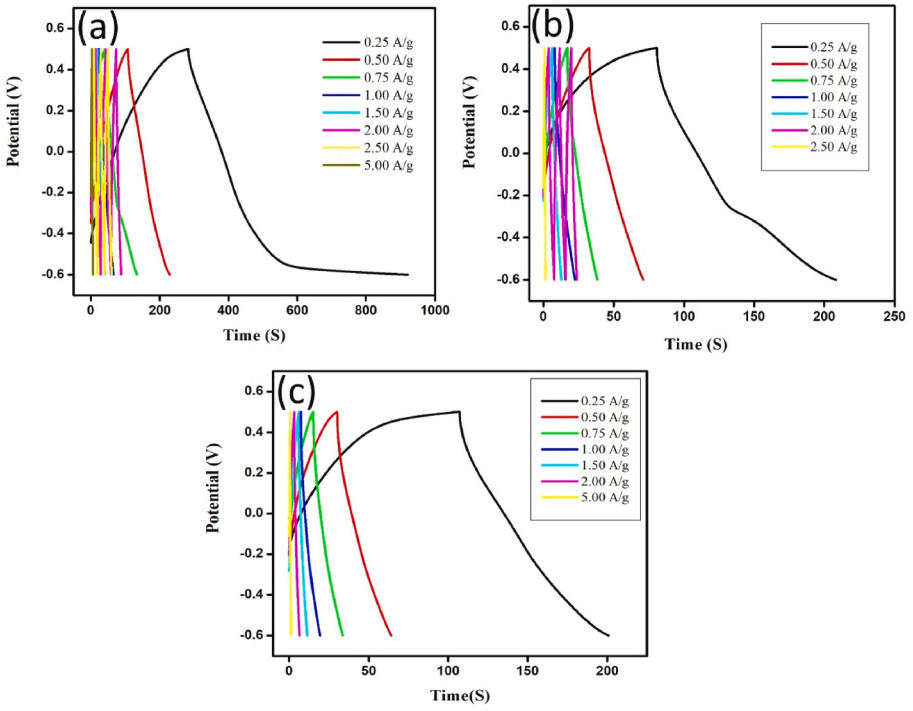


Fig. 7. GCD curve of $CuWO_4$ nanoparticles (a) 1:1 (b) 1:2 (c) 1:3.

plot exhibits a weak semicircular feature in the high-frequency region followed by an inclined straight line in the low-frequency region. The intercept at the real axis corresponds to the solution resistance (Rs), which is found to be 1.98 Ω, indicating low intrinsic resistance and good electrical conductivity. Due to the absence of a well-defined semicircle, precise estimation of the charge-transfer resistance (Rct) from the Nyquist plot is not reliable. However, the suppressed semicircular feature suggests a very low charge-transfer resistance and fast electron transfer kinetics at the electrode–electrolyte interface. Overall, the low Rs value and the observed impedance characteristics indicate reduced interfacial resistance, enhanced conductivity, and efficient charge transport, which collectively contribute to the improved

Table 1
Specific capacitance values of CuWO4 nanoparticles with different current density.

Current Density (A/g)	Cs (F/g) (a) 1:1	Cs (F/g) (b) 1:2	Cs (F/g) (c) 1:3
0.25	204.5	47.7	45.5
0.50	100.0	31.8	25.0
0.75	81.8	30.7	27.3
1.00	72.7	31.8	27.3
1.50	68.2	34.1	30.0
2.00	63.6	32.7	29.1
2.50	56.8	27.3	—
5.00	54.5	—	36.4

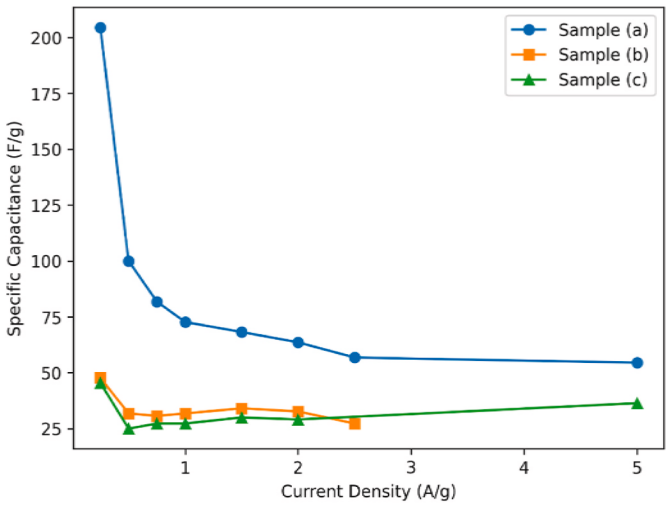


Fig. 8. Specific Capacitance vs Current density (a) 1:1 (b) 1:2 (c) 1:3.

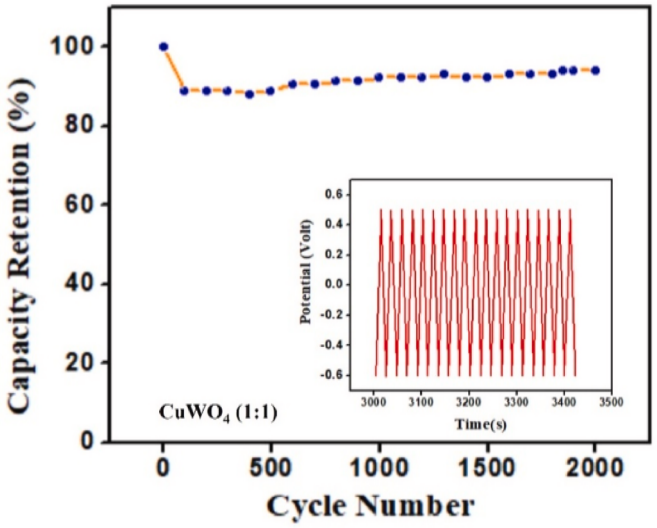


Fig. 9. Cyclic stability of $CuWO_4$ nanoparticles.

electrochemical performance of the $CuWO_4$ electrode.

5. Conclusion

This study demonstrates a clear correlation between structure, morphology, and electrochemical performance through the controlled synthesis of $CuWO_4$ nanoparticles with varying Cu:W ratios via a sol–gel

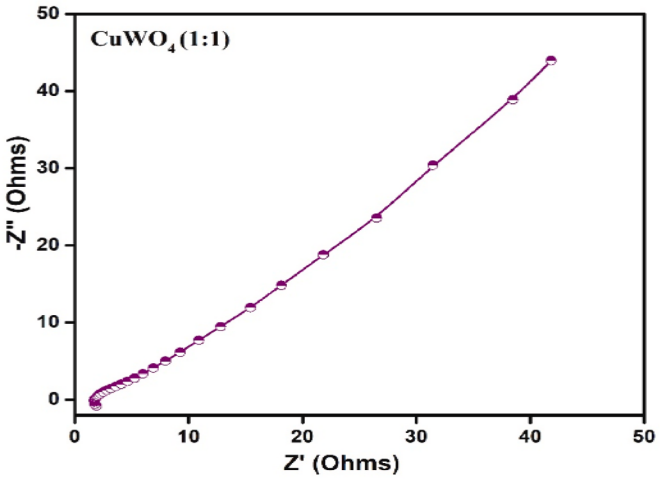


Fig. 10. Nyquist plot of $CuWO_4$ (1:1) nanoparticle.

method. XRD analysis confirms the successful formation of phase-pure, well-crystallized $CuWO_4$ without secondary phases, indicating effective incorporation of Cu and W into the lattice. SEM observations reveal uniformly distributed nanosized particles with an interconnected architecture, which facilitates efficient electrolyte penetration and ion transport. XPS results further verify the oxidation states of Cu^{2+}/Cu^{+} and W^{6+}, confirming the redox-active nature of the material, while EIS analysis demonstrates low solution resistance and charge transfer resistance, indicating enhanced conductivity and fast electron transfer kinetics. Electrochemical studies confirm pseudocapacitive behavior for all compositions; however, performance is strongly influenced by stoichiometry. The Cu:W (1:1) composition exhibits superior electrochemical performance due to an optimal balance between electrical conductivity and the availability of redox-active sites, along with improved ion diffusion enabled by the nanoscale morphology. In contrast, higher tungsten content leads to reduced conductivity and limited electrochemical utilization. Overall, this work highlights the critical role of stoichiometric control, structural integrity, and tailored morphology in optimizing charge storage behavior, providing valuable insights for the rational design of high-performance transition metal oxide-based supercapacitor electrodes.

Funding

The authors declare that no funds, grants, or other support were received during the preparation of this manuscript.

CRediT authorship contribution statement

S. Umera Sulthana: Data curation, Formal analysis, Methodology, Writing – original draft. **D. Sridevi:** Data curation, Formal analysis. **V. Balasubramanian:** Formal analysis, Investigation, Software, Writing – review & editing. **B. Shunmugapriya:** Formal analysis, Validation. **A. Alfind Paul Frit:** Supervision, Validation. **V. Gowthami:** Conceptualization, Supervision, Validation, Writing – review & editing.

Declaration of competing interest

The authors declare that they have no known competing financial interests or personal relationships that could have appeared to influence the work reported in this paper.

Acknowledgement

The authors would like to extend their warmest regards to the Vels

Institute of Science, Technology and Advanced studies, Chennai for providing the necessary facilities for carrying out the research work.

Data availability

Data will be made available on request.

References

[1] B.E. Conway, Electrochemical Supercapacitors: Scientific Fundamentals and Technological Applications, Kluwer Academic Publishers, 1990.
[2] G. Wang, L. Zhang, J. Zhang, A review of electrode materials for supercapacitors, Chem. Soc. Rev. 41 (2) (2012) 797–828.
[3] H. Li, L. Wang, J. Qiu, Transition metal tungstates for electrochemical energy storage, Nano Energy 36 (2017) 109–126.
[4] Y. Liu, J. Zhang, H. Liu, Morphology-controlled synthesis of $CuWO_4$ nanostructures for supercapacitors, Electrochim. Acta 265 (2018) 329–338.
[5] X. Wang, Y. Wang, Y. Xie, Nanostructured $CuWO_4$ as high-performance electrode material for supercapacitors, J. Power Sources 412 (2019) 159–167.
[6] X. Chen, Y. Zhou, Y. Zhang, Enhanced supercapacitive performance of $CuWO_4$@ carbon nanocomposites, Mater. Lett. 262 (2020) 113–117.
[7] L. Zhang, Z. Sun, Y. Li, $CuWO_4$-based nanostructures for energy storage applications, ACS Appl. Mater. Interfaces 13 (10) (2021) 12247–12256.
[8] Y. Wang, H. Zhang, J. Li, Conductive polymer composites with $CuWO_4$ for supercapacitors, Electrochim. Acta 338 (2020) 135887.
[9] W. Weng, Q. Zhang, X. Liu, Doping strategies to enhance $CuWO_4$ electrochemical performance, ACS Appl. Energy Mater. 4 (5) (2021) 4562–4572.
[10] Y. Zhang, Z. Sun, Y. Li, Surface engineering of $CuWO_4$ for improved electrochemical properties, Nano Energy 74 (2020) 104–112.
[11] X. Zhang, H. Zhou, Hierarchical $CuWO_4$ nanostructures for high-capacitance supercapacitors, Adv. Funct. Mater. 29 (35) (2019) 1903004.
[12] H. Liu, L. Wang, M. Chen, Electrochemical doping of $CuWO_4$: a pathway to enhanced supercapacitor performance, Electrochim. Acta 338 (2020) 135887.
[13] J. Wu, Z. Sun, Y. Li, Flexible supercapacitors based on $CuWO_4$ nanostructures, Carbon 174 (2021) 336–346.
[14] Q. Zhang, Y. Wang, Novel hybrid architectures of $CuWO_4$ with conductive polymers for supercapacitors, Adv. Mater. 34 (12) (2022) 2106887.
[15] Y. Zhang, et al., Recent advances in copper tungstate nanostructures for energy storage, Mater. Today Energy 20 (2021) 100747.
[16] A. Manohar, T. Suvarna, S.P. Vattikuti, B.A. Al-Asbahi, S. Sangaraju, N. Mameda, K.H. Kim, Synthesis, characterization and electrochemical properties of Ni0. 4Mg0. 6Fe2O4/CeO2/MnFe2O4 nanocomposite, Ceram. Int. 51 (5) (2025) 6525–6532.
[17] A. Manohar, T. Suvarna, S.P. Vattikuti, D. Kim, S. Sangaraju, B.A. Al-Asbahi, K. H. Kim, Zn0. 5MgxCu0.5-xFe2O4 spinel ferrites as electrode materials for supercapacitor applications, Inorg. Chem. Commun. 177 (2025) 114393.
[18] A. Meena, H. Saleem, A.S. Kumar, N. Shanmugam, M. Suganya, Stoichiometry-balanced MnO2/NiO nanoscale heterostructures for high-energy and high-power supercapacitors, Inorg. Chem. Commun. (2025) 115785.
[19] H. Wang, et al., Electrochemical properties of $CuWO_4$/graphene composites, Electrochim. Acta 345 (2020) 136184.
[20] J. Li, et al., Synthesis and electrochemical investigation of hierarchical $CuWO_4$ nanostructures, J. Alloys Compd. 798 (2019) 146–154.
[21] Z. Chen, et al., Surface modification strategies for copper tungstate-based supercapacitors, ACS Appl. Mater. Interfaces 13 (15) (2021) 17424–17433.
[22] X. Yu, et al., Doped $CuWO_4$ nanostructures for high-performance supercapacitors, Nano Energy 95 (2022) 107013.
[23] P. Zhao, et al., Future perspectives of tungstate-based electrode materials, Adv. Funct. Mater. 33 (5) (2023) 2207319.
[24] R.L. Frost, S.J. Palmer, B.J. Reddy, Raman spectroscopic study of wolframite-type tungstates, J. Raman Spectrosc. 34 (2003) 214–220.
[25] D. Errandonea, J. Pellicer-Porres, F.J. Manjón, et al., High-pressure structural and vibrational study of $CuWO_4$, Phys. Rev. B 79 (2009) 184104.
[26] X. Wang, Y. Li, C. Liu, et al., Structural and vibrational properties of nanostructured $CuWO_4$ investigated by Raman spectroscopy, J. Alloys Compd. 587 (2014) 679–684.
[27] H. Wang, L. Zhang, Z. Chen, et al., Structure–morphology–property relationship in $CuWO_4$ nanomaterials, J. Alloys Compd. 688 (2016) 108–115.
[28] Y. Liu, J. Guo, M. Yang, et al., Effect of composition on the microstructure and electrochemical behavior of metal tungstates, Ceram. Int. 45 (2019) 15632–15640.
[29] M.C. Biesinger, L.W. Lau, A.R. Gerson, R.S.C. Smart, Resolving surface chemical states in XPS analysis of first row transition metals, oxides and hydroxides: sc, Ti, V, Cu and Zn, Appl. Surf. Sci. 257 (2010) 887–898.
[30] O.Y. Khyzhun, T. Strunskus, S. Cramm, Y.M. Solonin, Electronic structure of CuWO4: XPS, XES and NEXAFS studies, J. Alloys Compd. 389 (1–2) (2005) 14–20.
[31] C. Wei, Y. Huang, X. Zhang, X. Chen, J. Yan, Soft-template hydrothermal systhesis of nanostructured copper (II) tungstate cubes for electrochemical charge storage application, Electrochim. Acta 220 (2016) 156–163.
[32] H. Chen, L. Hu, Y. Yan, R. Che, M. Chen, L. Wu, One-step synthesis of metal tungstate nanostructures and their application in supercapacitors, J. Mater. Chem. A 2 (2014) 826–835.
[33] J. Zhou, X. Li, Y. Zhao, J. Zhang, Enhanced electrochemical performance of transition-metal tungstate nanomaterials for supercapacitor applications, J. Power Sources 302 (2016) 393–401.
[34] H. Wang, H.S. Casalongue, Y. Liang, H. Dai, $Ni(OH)_2$ nanoplates grown on graphene as advanced electrochemical pseudocapacitor materials, J. Am. Chem. Soc. 132 (2010) 7472–7477.
[35] Y. Liu, X. Zhang, G. Wang, Transition metal tungstates as electrode materials for supercapacitors, Electrochim. Acta 176 (2015) 127–135.
[36] L. Zhang, H.B. Wu, X.W. Lou, Metal tungstate nanostructures for electrochemical energy storage, Adv. Energy Mater. 4 (2014) 1300958.
[37] A. Manohar, T. Suvarna, S.P. Vattikuti, P. Manivasagan, E.S. Jang, H.P. Sudhani, A. M. Al-Enizi, A. Kumar, K. Sharma, N. Mameda, K.H. Kim, Structural, morphological, magnetic, electrochemical and biocompatible properties of ZnFe2O4/MgFe2O4/NiFe2O4/CeO2 nanocomposites, Colloids Surf., A Physicochem. Eng. Asp. 705 (2025) 135667.
[38] A. Manohar, T. Suvarna, S.P. Vattikuti, J.P. Goud, B.A. Al-Asbahi, S.M. Qaid, N. Mameda, K.H. Kim, Investigating the potential of Mg0. 5ZnxCu0. 5-xFe2O4 nanoparticles for energy storage applications, Mater. Sci. Semicond. Process. 185 (2025) 108897.